

SCIENTIFIC REPORTS

OPEN

The High-Pressure Superconducting Phase of Arsenic

Prutthipong Tsuppayakorn-aek^{1,2,3}, Wei Luo³, Rajeev Ahuja^{3,4} & Thiti Bovornratanaraks^{1,2}

Ab initio random structure searching (AIRSS) technique is predicted a stable structure of arsenic (As). We find that the body-centered tetragonal (bct) structure with spacegroup $I4_1acd$ to be the stable structure at high pressure. Our calculation suggests transition sequence from the simple cubic (sc) structure transforms into the host-guest (HG) structure at 41 GPa and then into the bct structure at 81 GPa. The bct structure has been calculated using *ab initio* lattice dynamics with finite displacement method confirm the stability at high pressure. The spectral function α^2F of the bct structure is higher than those of the body-centered cubic (bcc) structure. It is worth noting that both bct and bcc structures share the remarkable similarity of structural and property. Here we have reported the prediction of temperature superconductivity of the bct structure, with a T_c of 4.2 K at 150 GPa.

The group-V element is one of central interest in a discipline in high-pressure physics and continues to attract a lot of attention as it has an incommensurate host-guest (HG) structure. The existence of a HG structure in the group-V elements is observed in As-III, Sb-IV, and Bi-III¹. They are a common high-pressure structure among the elemental metals. With increasing pressure, for As, a HG structure transforms into a body-centered cubic (bcc) structure at pressure 97 GPa. For Sb, a HG structure transforms into a bcc structure at pressure 28 GPa. For Bi, a HG structure transforms into a bcc structure at pressure 8 GPa. It is worth noting that the bcc crystal structure of them is the most stable structure at the highest pressure.

Arsenic (As) maintains the bcc crystal structure up to at least 122 GPa², the structural phase transition under high pressure is influenced by *s-d* hybridization from lower pressure to higher pressure phases³. At ambient pressure, As possesses a rhombohedral As-type (As-I) structure and transforms into a simple-cubic (As-II) structure at 25 GPa. At higher pressure, it transforms into a body-centered monoclinic host-guest (As-III) structure at 48 GPa, and then into a body-centered cubic (As-IV) at 97 GPa. Moreover, As is also presented by experimental study with superconducting transition temperature (T_c) of 2.5 K and 32 GPa⁴.

Several metals are superconducting at high pressure^{5–10}, with increasing pressure, it indicates that the superconducting transition temperature (T_c) is also increasing. A striking example of the group-II elements, Ca has been reported highest T_c among elemental metals, with a T_c of 29 K at 216 GPa⁵. Sr and Ba have been reported to possess a T_c of 8 K at 58 GPa⁶, and a T_c of 5 K at 18 GPa⁷, respectively. Moreover, the group-III elements, the T_c of Y has reached of 20 K at 115 GPa^{8,9} and Sc has also observed to possess a T_c of 19.8 K at 107 GPa⁹. Furthermore, the group-V element, As has reached a maximum T_c of 2.7 K at 24 GPa¹⁰, Sb has reported to possess a T_c of 3.6 K at 3.5 GPa¹⁰, and Bi has reported to possess the highest T_c among the group-V element, with the T_c of 8.7 K at 9 GPa¹⁰. Recently, Chan *et al.*¹¹ predicted the T_c of the simple cubic (sc) structure in the pressure range 30–50 GPa with the T_c as high as 2.99 K at 30 GPa. They also reported that the T_c of the sc structure decreases monotonically with increasing pressure T_c at 0.58 K and 50 GPa.

An important and a fundamental question remains to predict a new phase of As in the pressure range 100–300 GPa because there is no high-pressure phase beyond the bcc structure². Thus, the searching technique leads to the discovery of high-pressure As structure. In addition, there is no reported the T_c for the predicted structure in As. It would be interesting to investigate the role of electron-phonon coupling (EPC) in order to predict T_c at high pressure.

In this work, in order to understand the predicted structure at high pressures, it is important to obtain as much information as possible about the structure. Hence, there have also been opened questions for As under

¹Extreme Conditions Physics Research Laboratory (ECPR) and Physics of Energy Materials Research Unit (PEMRU), Department of Physics, Faculty of Science, Chulalongkorn University, Bangkok, 10330, Thailand. ²Thailand Center of Excellence in Physics, Commission on Higher Education, 328 Si Ayutthaya Road, Bangkok, 10400, Thailand.

³Condensed Matter Theory Group, Department of Physics, Uppsala University, Box 530, S-751 21, Uppsala, Sweden.

⁴Department of Materials and Engineering, Applied Materials Physics, Royal Institute of Technology (KTH), SE-100 44, Stockholm, Sweden. Correspondence and requests for materials should be addressed to R.A. (email: rajuv@physics.uu.se) or T.B. (email: thiti.b@chula.ac.th)

Received: 5 October 2017

Accepted: 12 January 2018

Published online: 14 February 2018

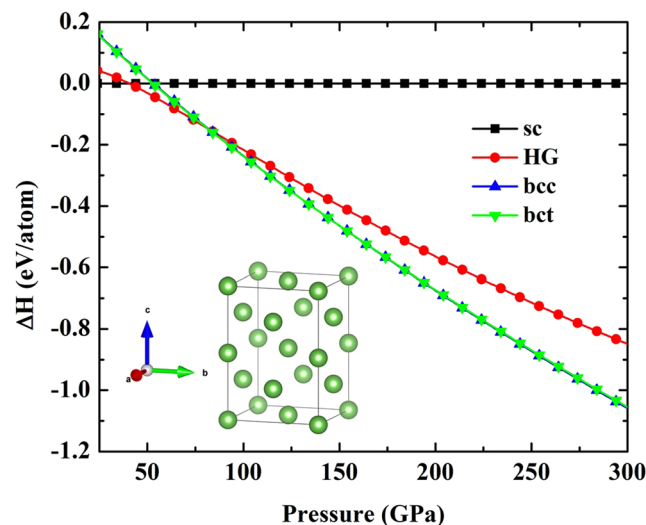


Figure 1. Comparison of the enthalpies of As phases up to 300 GPa. As structures relative to the sc structure at 0 K.

extreme compression: (i) what is a new structure beyond the bcc structure at high pressure? (ii) Is the metallic high-pressure phase a superconductor? In order to address these problems, we report a theoretical investigation of the theoretical prediction which presents a new lowest enthalpy phase of As.

Results and Discussion

Our calculation has searched at pressures above 100 GPa, we find the lowest enthalpy structure of As which is the body-centered tetragonal (bct) structure with spacegroup $I4_1/acd$. We also show that the simulated crystal structure of the bct structure is obtained as implemented in VESTA¹² (Fig. 1). The optimized structural parameters for the bct structure are $a = 4.072 \text{ \AA}$ and $c = 5.802 \text{ \AA}$ with As atoms located at 8 a symmetry site (0, 0.5, 0.25). In Fig. 1, we present the enthalpies of different As phases with respect to the sc structure which are plotted as a function of pressure. Crossing points of curve from each structure represent the sc structure transforms into the HG structure at 41 GPa and into the bct structure at 81 GPa as shown in Fig. 1.

With increasing pressure, the transition sequence is successfully observed by the experimental study¹. The low-pressure sc structure of As transforms into the monoclinic host-guest (HG) structure at pressure 48 GPa, and then into the body-centered cubic (bcc) structure at pressure 97 GPa¹. On the contrary, our calculation proposes that transition sequence should be from the sc structure transforms into the HG structure at pressure 41 GPa and then into the bct structure at 81 GPa. Moreover, we show that the bcc and bct structures of As are very close in enthalpy which the bct structure has only slightly lower enthalpy than the bcc structure by 1 meV/atom.

Interesting, the bcc structure is the super-spacegroup ($Im\bar{3}m$) and the bct structure is sub-spacegroup ($I4_1/acd$) of the bcc structure which suggests that the bct structure is a possible coexistence phase with the bcc structure. Our enthalpy calculation reveal that both the bcc and bct structures are remarkably closed overpressure range 100 to 300 GPa.

In fact, the bcc and bct structures have very similar crystal structures. In order to determine difference between the bcc and bct structures, Fig. 2 shows a comparison of crystal structures by simulating powder diffraction patterns at 100 GPa. The peak 200, 211, 220, and 310 of the bct structure are distorted from the bcc structure because the bct index peaks split into two peaks with respect the bcc structure. The bct has been confirmed with slightly distorted parameter a/c lowered by 1% with respect to the bcc structure.

This calculation leads to a new stable structure, we identify the dynamic stability of the bct structure by the phonon dispersion relation. The lack of imaginary frequencies provides a confirmation that the bct structure is stable at pressure 300 GPa (Fig. 3).

In the whole pressure interval of 150–300 GPa, we use a fixed value for the effective Coulomb interaction parameter. It is worth noting that the value of effective Coulomb interaction parameter also used $\mu^* = 0.10$, which is assumed for all metals by Allen and Dynes¹³. In fact, the μ^* plays an important role to give the T_c at high pressure. Especially, the nature of As is observed that the T_c is decreased with increasing pressure through the evolution of μ^* ¹¹. We also explored the effects on T_c of changing μ^* from 0.10 to 0.18^{13–15} at 150 GPa as shown in Table 1 Thus, we did consider the effect of $\mu^* = 0.10$ on the predicted T_c because it gives the highest T_c among the evolution of μ^* . Our prediction concerning the superconducting phase of As at high pressures would be experimentally confirmed. At 150 GPa, the spectral function α^2F of the bct structure is higher than those of the bcc structure around frequency region 6–13 THz. Likewise, the integrated λ of the bct structure is also higher than the bcc structure (Fig. 4). Moreover, it exhibits the metallization and it predicts to give temperature superconductivity in the bct structure, with the T_c of 4.2 K at 150 GPa as can be seen Fig. 5.

At high pressure, pressure-induced superconductivity shown in Fig. 5. We also explore the effects on T_c of increasing pressure. Our calculations reveal T_c both the bcc and bct structures with increasing pressure, which

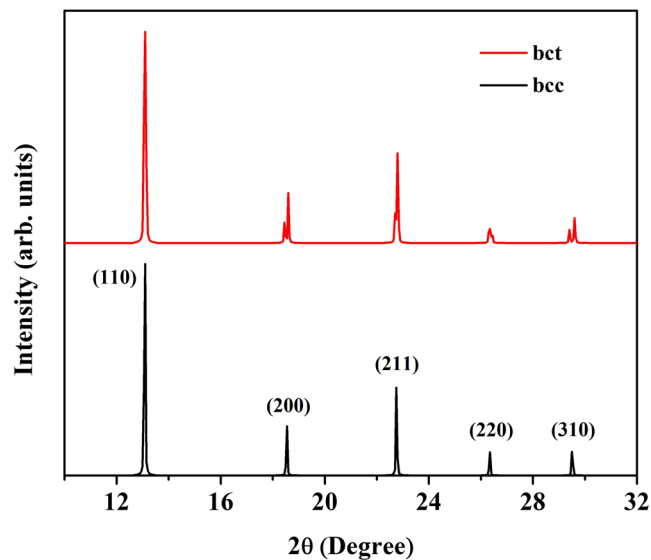


Figure 2. Simulated x-ray powder diffraction patterns of the bcc structure (black) and the bct structure (red).

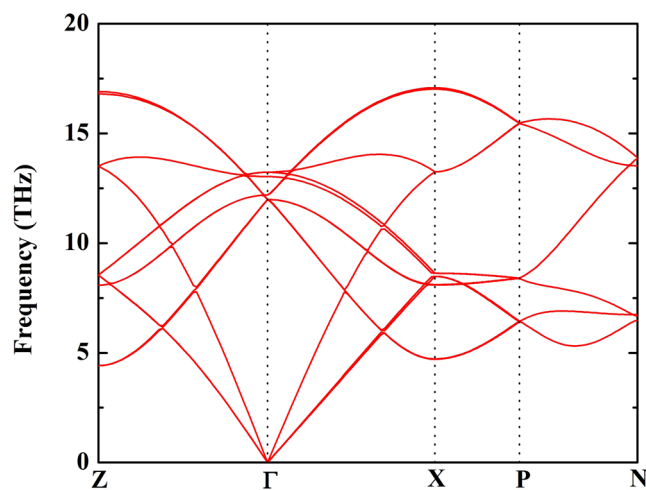


Figure 3. The dynamical harmonic stabilization of the bct structure at pressure 300 GPa.

Structures	T _c (K)			
	$\mu^* = 0.10$	$\mu^* = 0.13$	$\mu^* = 0.15$	$\mu^* = 0.18$
bct	4.2	2.5	1.6	0.7
bcc	3.4	2.0	1.3	0.5

Table 1. Calculated effective Coulomb interaction parameter μ^* , and superconducting transition temperature T_c for As at 150 GPa.

generally shows monotonic decreasing behaviours. Especially, the λ of the bct structure is higher than the bcc structure at 150 GPa which has led to suggestions for possible the highest T_c of the bct structure. It indicates that the T_c of the bct structure is higher than the bcc structure, where it possesses the highest T_c of 4.2 K.

Above 150 GPa, we find that the T_c of the bct structure is lower than the bcc structure as well as T_c gradually decreases with pressure. We calculate λ and the averaged phonon frequency (ω_{log}) as a function of pressure of the bcc and bct structures. The λ of the bcc and bct structures decrease monotonically between 150 GPa and 300 GPa, respectively. The ω_{log} of the bcc and bct structures increase monotonically between 150 GPa and 300 GPa, respectively as can be seen the inset in Fig. 5.

Moreover, we strongly suggested that the bct structure is not superconducting phase above 300 GPa. This is due to the fact that the bct structure remains in the metallic state at 300 GPa, we propose that it becomes a normal metallic state since the λ of the bct structure is poorly characterized, with increasing pressure. It should be noted that the λ is weakly coupling for calculation the T_c . Here again, the μ^* plays a key role, in the sense that the

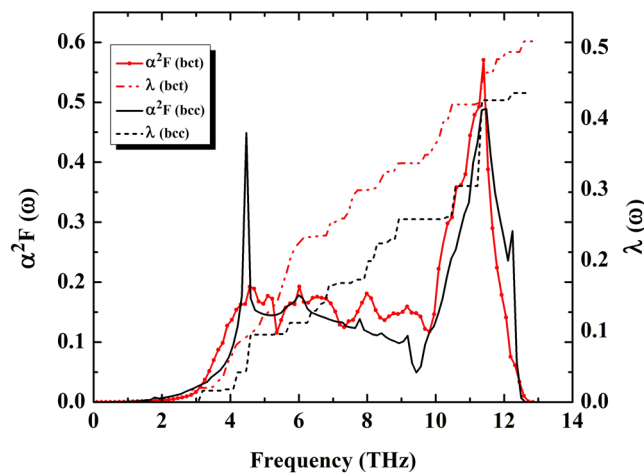


Figure 4. Spectral function $\alpha^2F(\omega)$ and integrated λ as a function of frequency of As at pressure 150 GPa.

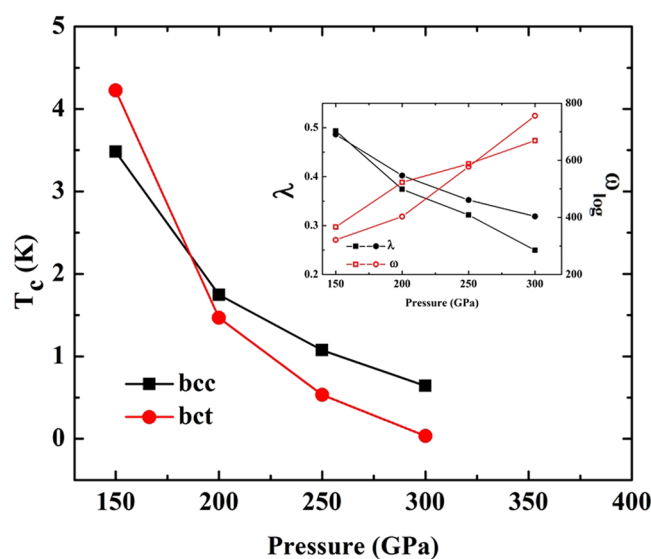


Figure 5. Superconducting T_c of As as a function of pressure. The square and the circle symbols represent calculations for the bcc and bct structures, respectively. The inset shows calculated electron-phonon coupling for the bcc structure (filled square) and the bct structure (filled circle) and averaged phonon frequency as a function of pressure for the bcc structure (hollow square) and the bct structure (hollow circle).

increasing pressure induces the T_c of the bct structure decreasing. This might lead to new interpretation of the experimental data above 150 GPa.

Conclusion

In conclusion, the AIRSS technique reveals the new stable bct structure with spacegroup $I4_1/acd$ of As at high pressure. We show that structural phase transformation of As from sc to HG to bct at 41, and 81 GPa, respectively. We confirm that bct is thermodynamically stable above 81 GPa and our result show that it is also dynamically stable at 300 GPa. Therefore, we suggest the transitions sequence from the sc structure transforms into the HG structure at 41 GPa and then into the bct structure at 81 GPa. We find that the T_c of the bct structure is the maximum around 4.2 K at 150 GPa. It is worth noting that from our calculation both bct and bcc structures share remarkable similarity in structural and property. Thus, both structures may be observed by experimental at low temperature and high pressure.

Methods

We used *ab initio* random structure searching (AIRSS) technique^{16,17} and *ab initio* calculation of the Cambridge Serial Total Energy Package (CASTEP)¹⁸ to predict the candidate crystal structures of As under pressure. The AIRSS technique is used to predict the crystal structures of materials^{16,17,19–22}. A plane-wave basis-set energy cut-off of 280 eV and an initial Brillouin-zone (BZ) sampling grid of spacing $2\pi \times 0.07 \text{ \AA}^{-1}$ were used for this calculation. The generalized gradient approximation (GGA) with the Perdew-Burke-Ernzerhof (PBE) parametrization²³

for the exchange–correlation functional was used for the structure searching. The AIRSS technique generated unit cells of random shapes with reasonable volumes.

We studied simulation cells containing 2, 4, 6, 8, 10, and 12 atoms of As at pressure 100, 150, 200, 250, and 300 GPa. The cell shapes and atomic positions are then relaxed to the ground state structure at each pressure. The AIRSS technique calculated the enthalpies of the phases at any pressure by using the simple linear approximation¹⁷.

$$H(p) \simeq H(p_s) + V_s(p - p_s), \quad (1)$$

Where p is any pressure and V_s is the volume of the phase at p_s . The quantities $H(p_s)$, p_s and V_s are calculated for each relaxed into higher-symmetry space groups obtained in a search.

We are here presented electronic structure by using the GGA-PBE²³ for the exchange–correlation functional to density functional theory. We employed the projector augmented wave (PAW) method²⁴, as implemented in the Vienna ab initio simulation package (VASP)²⁵. The PAW potential with a 15-electron ($3d^{10}4s^24p^3$) for As has been employed with plane waves basis set up to a cutoff energy of 500 eV and the initial BZ sampling grid of spacing $2\pi \times 0.02 \text{ \AA}$.

All structures were relaxed and their equations of state were obtained by fitting to the calculated energy–volume data with the third-order Birch–Murnaghan equation. We then calculated the enthalpy–pressure relationship and the high pressure phase from the experimental information¹.

The phonon dispersion of candidate structure was calculated by *ab initio* lattice dynamics with finite displacement method, as implemented in VASP code and the phonopy package²⁶.

We calculated the EPC with density functional perturbation theory²⁷. The plan waves basis set was expanded with a kinetic energy cutoff of 60 Ry. The calculation studies presented here are based on the GGA-PBE. We employed PAW method as implemented in Quantum Espresso²⁸. The BZ integrations in the electronic and phonon calculations were performed using MP meshes. Both the meshes of k-points for electronic states and the meshes of phonons were used in these calculation. For As-IV, individual phonon calculations were performed on the first BZ on $4 \times 4 \times 4$ q-meshes with a $12 \times 12 \times 12$ k-points mesh. For high-pressure candidate structure, individual phonon calculations were performed on the first BZ on $4 \times 4 \times 4$ q-meshes with a $8 \times 8 \times 8$ k-points mesh. For As-IV, The EPC matrix elements were computed in the first BZ on $4 \times 4 \times 4$ q-meshes using individual EPC matrices obtained with a $24 \times 24 \times 24$ k-points mesh. For the bct structure, The EPC matrix elements were computed in the first BZ on $4 \times 4 \times 4$ q-meshes using individual EPC matrices obtained with a $16 \times 16 \times 16$ k-points mesh. We calculated T_c using the Allen–Dynes equation¹³, which is corresponded for $\lambda < 1.4$,

$$T_c = \frac{\omega_{log}}{1.2} \exp\left[-\frac{1.04(1 + \lambda)}{\lambda - \mu^*(1 + 0.62\lambda)}\right], \quad (2)$$

where ω_{log} is the averaged phonon frequency. We used effective Coulomb interaction parameter $\mu^* = 0.10$. It is assumed by the original Allen–Dynes formula¹³.

References

- Degtyareva, O., McMahan, M. I. & Nelves, R. J. High-pressure structural studies of group-15 elements. *High Pressure Research* **24**, 319–356, <https://doi.org/10.1080/08957950412331281057> (2004).
- Greene, R. G., Luo, H. & Ruoff, A. L. bcc arsenic at 111 gpa: An x-ray structural study. *Phys. Rev. B* **51**, 597–600, <https://doi.org/10.1103/PhysRevB.51.597> (1995).
- Häussermann, U., Söerberg, K. & Norrestam, R. Comparative study of the high-pressure behavior of as, sb, and bi. *Journal of the American Chemical Society* **124**, 15359–15367, <https://doi.org/10.1021/ja020832s> (2002).
- Chen, A. L., Lewis, S. P., Su, Z., Yu, P. Y. & Cohen, M. L. Superconductivity in arsenic at high pressures. *Phys. Rev. B* **46**, 5523–5527, <https://doi.org/10.1103/PhysRevB.46.5523> (1992).
- Sakata, M., Nakamoto, Y., Shimizu, K., Matsuoka, T. & Ohishi, Y. Superconducting state of ca-vii below a critical temperature of 29 k at a pressure of 216 gpa. *Phys. Rev. B* **83**, 220512, <https://doi.org/10.1103/PhysRevB.83.220512> (2011).
- Mizobata, S., Matsuoka, T. & Shimizu, K. Pressure dependence of the superconductivity in strontium. *Journal of the Physical Society of Japan* **76**, 23–24 (2007).
- Dunn, K. J. & Bundy, F. P. Pressure-induced superconductivity in strontium and barium. *Phys. Rev. B* **25**, 194–197, <https://doi.org/10.1103/PhysRevB.25.194> (1982).
- Hamlin, J., Tissen, V. & Schilling, J. Superconductivity at 20 k in yttrium metal at pressures exceeding 1 mbar. *Physica C: Superconductivity and its Applications* **451**, 82–85, <http://www.sciencedirect.com/science/article/pii/S0921453406008082>. <https://doi.org/10.1016/j.physc.2006.10.012> (2007).
- Debessai, M., Hamlin, J. J. & Schilling, J. S. Comparison of the pressure dependences of T_c in the trivalent d -electron superconductors sc, y, la, and lu up to megabar pressures. *Phys. Rev. B* **78**, 064519, <https://doi.org/10.1103/PhysRevB.78.064519> (2008).
- Buzza, C. & Robbie, K. Assembling the puzzle of superconducting elements: a review. *Superconductor Science and Technology* **18**, R1, <http://stacks.iop.org/0953-2048/18/i=1/a=R01> (2005).
- Chan, K. T., Malone, B. D. & Cohen, M. L. Electron–phonon coupling and superconductivity in arsenic under pressure. *Phys. Rev. B* **86**, 094515, <https://doi.org/10.1103/PhysRevB.86.094515> (2012).
- Momma, K. & Izumi, F. VESTA3 for three-dimensional visualization of crystal, volumetric and morphology data. *Journal of Applied Crystallography* **44**, 1272–1276, <https://doi.org/10.1107/S0021889811038970> (2011).
- Allen, P. B. & Dynes, R. C. Transition temperature of strong-coupled superconductors reanalyzed. *Phys. Rev. B* **12**, 905–922, <https://doi.org/10.1103/PhysRevB.12.905> (1975).
- McMillan, W. L. Transition temperature of strong-coupled superconductors. *Phys. Rev.* **167**, 331–344, <https://doi.org/10.1103/PhysRev.167.331> (1968).
- Kim, D. Y. & Ahuja, R. Ab initio study on pressure-induced change of effective coulomb interaction in superconducting yttrium. *Applied Physics Letters* **96**, 022510, <https://doi.org/10.1063/1.3291050> (2010).
- Pickard, C. J. & Needs, R. J. High-pressure phases of silane. *Phys. Rev. Lett.* **97**, 045504, <https://doi.org/10.1103/PhysRevLett.97.045504> (2006).

17. Pickard, C. J. & Needs, R. J. Ab initio random structure searching. *Journal of Physics: Condensed Matter* **23**, 053201, <http://stacks.iop.org/0953-8984/23/i=5/a=053201> (2011).
18. Clark, S. J. *et al.* First principles methods using CASTEP. *Z. Kristall.* **220**, 567–570 (2005).
19. Pickard, C. J. & Needs, R. J. Dense low-coordination phases of lithium. *Phys. Rev. Lett.* **102**, 146401, <https://doi.org/10.1103/PhysRevLett.102.146401> (2009).
20. Pickard, C. J., Martinez-Canales, M. & Needs, R. J. Density functional theory study of phase iv of solid hydrogen. *Phys. Rev. B* **85**, 214114, <https://doi.org/10.1103/PhysRevB.85.214114> (2012).
21. Pickard, C. J., Martinez-Canales, M. & Needs, R. J. Decomposition and terapascal phases of water ice. *Phys. Rev. Lett.* **110**, 245701, <https://doi.org/10.1103/PhysRevLett.110.245701> (2013).
22. Errea, I. *et al.* High-pressure hydrogen sulfide from first principles: A strongly anharmonic phonon-mediated superconductor. *Phys. Rev. Lett.* **114**, 157004, <https://doi.org/10.1103/PhysRevLett.114.157004> (2015).
23. Perdew, J. P., Burke, K. & Ernzerhof, M. Generalized gradient approximation made simple. *Phys. Rev. Lett.* **77**, 3865–3868, <https://doi.org/10.1103/PhysRevLett.77.3865> (1996).
24. Blöchl, P. E. Projector augmented-wave method. *Phys. Rev. B* **50**, 17953–17979, <https://doi.org/10.1103/PhysRevB.50.17953> (1994).
25. Kresse, G. & Furthmüller, J. Efficient iterative schemes for *ab initio* total-energy calculations using a plane-wave basis set. *Phys. Rev. B* **54**, 11169–11186, <https://doi.org/10.1103/PhysRevB.54.11169> (1996).
26. Togo, A. & Tanaka, I. First principles phonon calculations in materials science. *Scr. Mater.* **108**, 1–5 (2015).
27. Baroni, S., de Gironcoli, S., Dal Corso, A. & Giannozzi, P. Phonons and related crystal properties from density-functional perturbation theory. *Rev. Mod. Phys.* **73**, 515–562, <https://doi.org/10.1103/RevModPhys.73.515> (2001).
28. Giannozzi, P. *et al.* Quantum espresso: a modular and open-source software project for quantum simulations of materials. *Journal of Physics: Condensed Matter* **21**, 395502, <http://stacks.iop.org/0953-8984/21/i=39/a=395502> (2009).

Acknowledgements

We gratefully acknowledge Swedish National Infrastructure for Computing (SNIC) and High Performance Computing Center North (HPC2N) for providing computing time. P.T. thanks the Erasmus Mundus project (EXPERTS SUSTAIN project) for offering scholarships in the academic year 2016/2017, Thailand Center of Excellence in Physics (ThEP), and 90th Year Chulalongkorn Scholarship. This work has been partially supported by Super SCI-II research grant, Faculty of Science and Ratchadaphiseksomphot Endowment Fund of Chulalongkorn University (CU-59-039-AM). T.B. acknowledge Thailand Research Fund contract number RSA5880058.

Author Contributions

Author contributions: P.T., R.A., and T.B. designed research; P.T. and W.L. performed research; P.T., W.L., R.A., and T.B. analyzed data; and P.T., W.L., R.A., and T.B. wrote the paper.

Additional Information

Competing Interests: The authors declare no competing interests.

Publisher's note: Springer Nature remains neutral with regard to jurisdictional claims in published maps and institutional affiliations.



Open Access This article is licensed under a Creative Commons Attribution 4.0 International License, which permits use, sharing, adaptation, distribution and reproduction in any medium or format, as long as you give appropriate credit to the original author(s) and the source, provide a link to the Creative Commons license, and indicate if changes were made. The images or other third party material in this article are included in the article's Creative Commons license, unless indicated otherwise in a credit line to the material. If material is not included in the article's Creative Commons license and your intended use is not permitted by statutory regulation or exceeds the permitted use, you will need to obtain permission directly from the copyright holder. To view a copy of this license, visit <http://creativecommons.org/licenses/by/4.0/>.

© The Author(s) 2018